STRESS WORK EFFECT ON NATURAL CONVECTION FLOW ALONG A VERTICAL FLAT PLATE WITH JOULE HEATING AND HEAT CONDUCTION

Md. M. Alam
Department of Mathematics
Dhaka University of Engineering and Technology, Gazipur-1700, Bangladesh
M. A. Alim* and Md. M. K. Chowdhury
Department of Mathematics, Bangladesh University of Engineering and Technology,
Dhaka-1000, Bangladesh
*Corresponding email: maalim@math.buet.ac.bd

Abstract: *In the present paper, the effects of viscous dissipation and pressure stress work on free convection flow along a vertical plate have been investigated. Joule heating and heat conduction through a wall of finite thickness are considered in the investigation. With a goal to attain similarity solutions of the problem, the developed equations are made dimensionless by using suitable transformations. The non-dimensional equations are then transformed into non-similar forms by introducing non- similarity transformations. The resulting non-similar equations together with their corresponding boundary conditions based on conduction and convection are solved numerically by using the finite difference method along with Newton's linearization approximation. Numerically calculated velocity profiles, temperature profiles, skin friction coefficient and the surface temperature distributions are shown both on graphs and tables for different values of the parameters entering into the problem.*

Keywords: *Free convection, Joule heating, viscous dissipation and pressure work.*

INTRODUCTION

Free convection flow is often encountered in cooling of nuclear reactors or in the study of the structure of stars and planets. Along with the free convection flow, the phenomenon of the boundary layer flow of an electrically conducting fluid up a vertical flat plate in presence of joule heating and magnetic field is also very common because of their applications in nuclear engineering in connection with the cooling of reactors. Ackroyd[(1)] studied the stress work effects in laminar flat plate natural convection flow. Free convection from a vertical permeable circular cone with pressure work and non-uniform surface temperature has been illustrated by Alam et al.[(2)]. In a subsequent paper [(3)], they studied the effect of pressure stress work and viscous dissipation in natural convection flow along a vertical flat plate with heat conduction. Combined effect of viscous dissipation and Joule heating on the coupling of conduction and free convection along a vertical flat plate has been studied by Alim et al.[(4)]. Gebhart[(5)] has shown that the viscous dissipation effect plays an important role in natural convection in various devices which are subjected to large deceleration or which operate at high rotational speeds and also in strong gravitational field processes on large scales (on large planets) and in geological processes. Joshi and Gebhart[(6)] have shown the effect of pressure stress work and viscous dissipation in some natural convection flows. Miyamoto et al.[(7)] studied the effect of axial heat conduction in a vertical flat plate on free convection heat transfer. Pozzi and Lupo[(8)] have shown the coupling of conduction with laminar natural convection along a flat plate.

With this understanding Takhar and Soundalgekar[(9)] have studied the effects of viscous and Joule heating on the problem posed by Sparrow and Cess[(10)], using the series expansion method of Gebhart[(5)]. Zakerullah[(11)] investigated the viscous dissipation and pressure work effects in axisymmetric natural convection flows. In the present work, we have investigated the viscous dissipation and pressure effect on the skin friction and the surface temperature distribution on a vertical flat plate placed in a

Nomenclature

B	plate thickness	$\bar{u}, \bar{v}$	velocity components
c_p	specific heat	u, v	dimensionless velocity components
d	$(T_b - T_\infty)/ T_\infty$	$\bar{x}, \bar{y}$	Cartesian coordinates
f	dimensionless stream function	x, y	dimensionless Cartesian coordinates
g	acceleration due to gravity		
h	dimensionless temperature	***Greek symbols***	
$\boldsymbol{J}$	Joule heating parameter		
$\boldsymbol{L}$	reference length, $\nu^{2/3}/g^{1/3}$	β	coefficient of thermal expansion
l	length of the plate	ε	pressure work parameter
$\boldsymbol{N}$	viscous dissipation parameter	η	dimensionless similarity variable
p	coupling parameter, $p = (\kappa_f/\kappa_s)(b/L)d^{1/4}$	κ_f, κ_s	fluid and solid thermal conductivities
$\boldsymbol{Pr}$	Prandtl number	μ, ν	dynamic and kinematic viscosities of the fluid
$\boldsymbol{T}$	temperature	θ	dimensionless temperature
T_b	temperature at outer surface of the plate	ρ	density of the fluid
T_s	solid temperature	σ	electrical conductivity
T_∞	fluid asymptotic temperature	ψ	stream function

viscous incompressible and electrically conducting fluid in presence of Joule-heating.

The transformed non similar boundary layer equations together with the boundary conditions based on conduction and convection were solved numerically using the implicit finite difference method with Keller box scheme by Keller[12] along with Newton's linearization approximation method. We have studied the effect of the Prandtl number *Pr,* the viscous dissipation parameter *N*, the Joule-heating parameter *J* and the pressure work parameter ε on the velocity and temperature fields as well as on the skin friction and surface temperature. The calculation is carried out for a fluid with low Prandtl number i.e., liquid metals.

GOVERNING EQUATIONS OF THE FLOW

Consider the steady two dimensional laminar free convection boundary layer flow of a viscous incompressible and electrically conducting fluid along a side of a vertical flat plate of thickness '*b*' insulated on the edges with temperature T_b maintained on the other side in the presence of a uniformly distributed transverse magnetic field. The flow configuration and the coordinate system are shown in figure 1.

The mathematical statement of the basic conservation laws of mass, momentum and energy for the steady viscous incompressible and electrically conducting flow are given as

$$\Delta\cdot\vec{q}=0 \tag{1}$$

$$\rho\ (\vec{q}.\nabla\ )\ \vec{q}=-\ \nabla p\ +\mu\ \nabla^2\vec{q}+\vec{J}\times\vec{B}\ +\vec{F} \tag{2}$$

$$\rho C_p\left(\vec{q}.\nabla\right)T-\left(\vec{q}.\nabla\right)P=\nabla.\left(\kappa\nabla T\right)+\left(\vec{J}\times\vec{B}\right)u+\mu\phi \tag{3}$$

Where $\vec{q}=(\bar{u},\bar{v})$, $\bar{u}$ and $\bar{v}$ are the velocity components along the $\bar{x}$ and $\bar{y}$ axes, respectively, $\vec{F}$ is the body force per unit volume which is defined as $-\rho g$, the terms $\vec{J}$ and $\vec{B}$ are respectively the current density and magnetic induction vector and the term $\vec{J}\times\vec{B}$ is the force on the fluid per unit volume produced by the interaction of the current and magnetic field in the absence of excess charges, T is the temperature of the fluid in the boundary layer , g is the acceleration due to gravity, κ is the thermal conductivity and C_p is the specific heat at constant pressure and μ is the viscosity of the fluid, $\vec{B}=\mu_e B_0$, μ_e being the magnetic permeability of the fluid and B_0 is the uniformly distributed transverse magnetic field of strength. In the energy equation the viscous dissipation, pressure work and Joule heating terms are included. After introducing the Ohm's law for current density-velocity, $\vec{J}=\sigma\left(\vec{q}\times\vec{B}\right)$ and the Boussinesq approximation, $\rho=\rho_\infty\left[1-\beta\left(T-T_\infty\right)\right]$ the basic equations (1) to (3) become:

$$\frac{\partial\bar{u}}{\partial\bar{x}}+\frac{\partial\bar{v}}{\partial\bar{y}}=0 \tag{4}$$

$$\bar{u}\frac{\partial\bar{u}}{\partial\bar{x}}+\bar{v}\frac{\partial\bar{u}}{\partial\bar{y}}=\nu\frac{\partial^2\bar{u}}{\partial\bar{y}^2}+g\beta\left(T-T_\infty\right)-\frac{\sigma B_0^2\bar{u}}{\rho} \tag{5}$$

$$\bar{u}\frac{\partial T}{\partial\bar{x}}+\bar{v}\frac{\partial T}{\partial\bar{y}}=\frac{\kappa}{\rho\ c_p}\frac{\partial^2 T}{\partial\bar{y}^2}+\frac{\nu}{c_p}(\frac{\partial\bar{u}}{\partial\bar{y}})^2+\frac{T\beta\ \bar{u}}{\rho C_p}\frac{\partial P}{\partial\bar{x}}+\frac{\sigma B_0^2}{\rho C_p}\bar{u}^2 \tag{6}$$

The appropriate boundary conditions to be satisfied by the above equations are

$$u=0, v=0 \text{ at } \bar{y}=0$$
$$u\to 0, T\to T_\infty \text{ as } \bar{y}\to\infty \tag{7}$$

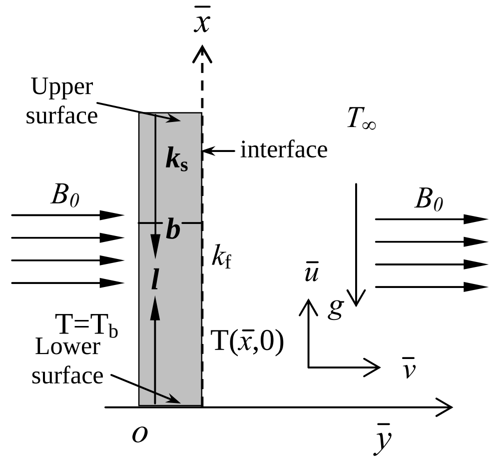

Figure 1: Physical configuration and coordinates system.

The temperature and the heat flux are considered continuous at the interface for the coupled conditions as given by Miyamoto et al.[7]. That is, at the interface,

$$\frac{k_s}{k_f}\frac{\partial T_{so}}{\partial\bar{y}}=(\frac{\partial T}{\partial\bar{y}})_{\bar{y}=0} \tag{8}$$

Where k_s and k_f are the thermal conductivities of the solid and the fluid, respectively. The temperature T_{so} in the solid is given by Pozzi and Lupo[8] as

$$T_{so}=T(x,0)-\{T_b-T(x,0)\}\frac{\bar{y}}{b} \tag{9}$$

Where $T(x,0)$ is the unknown temperature at the interface to be determined from the solutions of the equations. We observe that the equations (4)-(6) together with the boundary conditions (8)-(9) are non-linear partial differential equations, which have been solved numerically and are described in the following sections.

TRANSFORMATION OF THE EQUATIONS

Equations (4)–(6) may now be non-dimensionalized by using the following dimensionless variables:

$$x=\frac{\bar{x}}{L},\ y=\frac{\bar{y}}{L}d^{1/4},\ \bar{u}=\frac{\nu}{L}d^{1/2}u,\ \bar{v}=\frac{\nu}{L}d^{1/4}v,\ \theta=\frac{T-T_\infty}{T_b-T_\infty}$$
$$L=\frac{\nu^{2/3}}{g^{1/3}},\ d=\beta(T_b-T_\infty) \tag{10}$$

As the problem of natural convection, has no characteristic length, L has been defined in terms of ν and g that are the intrinsic properties of the system. The reference length along the 'y' direction has been modified by a factor $d^{-1/4}$ in order to eliminate this quantity from the dimensionless equations and the boundary conditions. For exterior conditions, we know hydrostatic pressure, $\partial P/\partial x=-\rho_e g$ and $\rho=\rho_e$, and the pressure work parameter $\varepsilon=(g\beta x)/C_P$ which is less than one as suggested by Gebhart[5]. Using the above relations (10), the non-dimensional form of the governing equations are:

$$\frac{\partial u}{\partial x}+\frac{\partial v}{\partial y}=0 \tag{11}$$

$$u\frac{\partial u}{\partial x}+v\frac{\partial u}{\partial y}+Mu=\frac{\partial^2 u}{\partial y^2}+\theta \tag{12}$$

$$u\frac{\partial\theta}{\partial x}+v\frac{\partial\theta}{\partial y}=\frac{1}{\Pr}\frac{\partial^2\theta}{\partial y^2}+N(\frac{\partial u}{\partial y})^2+J\,u^2-\frac{g_x\,\beta\left\{T_\infty+\left(T_b-T_\infty\right)\theta\right\}}{C_p\left(T_b-T_\infty\right)} \tag{13}$$

Where P_r = $\mu C_p / \kappa_f$ is the Prandtl number, J = $\sigma B_0^2 \nu d^{1/2} / \rho C_p (T_b - T_\infty)$ is the Joule-heating parameter and N = $\nu^2 d / L^2 c_p (T_b - T_\infty)$ is the dimensionless viscous dissipation parameter.

The corresponding boundary conditions (7) - (8) take the following form:

$$u = v = 0\ ,\ \theta - 1 = p\frac{\partial \theta}{\partial y} \quad \text{at } y = 0 \tag{14}$$

$$u \to 0,\ v \to 0 \quad \text{as } y \to \infty \tag{15}$$

where P is the pressure and p is the conjugate conduction parameter given by p = (κ_f / κ_s) (b/L) $d^{1/4}$. Here, the coupling parameter 'p' governs the described problem. The order of magnitude of 'p' depends actually on b/L and κ_f / κ_s , $d^{1/4}$ being the order of unity. The term b/L attains values much greater than one because of L being small. In case of air, κ_f / κ_s becomes very small when the vertical plate is highly conductive i.e. $\kappa_s >> 1$ and for materials, O(κ_f / κ_s) = 0.1 such as glass. Therefore, in different cases 'p' is different but not always a small number. In the present investigation, we considered p = 1 which is accepted for b/L of O(κ_f / κ_s). To solve the equations (11) – (13) subject to the boundary conditions (14) to (15), the following transformations were introduced for the flow region starting from up stream to down stream.

$$\psi = x^{4/5}(1+x)^{-1/20} f(x,\eta),\ \ \eta = yx^{-1/5}(1+x)^{-1/20},\ \ \theta = x^{1/5}(1+x)^{-1/5} h(x,\eta) \tag{16}$$

Here η is the dimensionless similarity variable and $h(x, \eta)$ is the dimensionless temperature. ψ is the stream function which satisfies the equation of continuity and $u = \frac{\partial \psi}{\partial y}$ *and* $v = -\frac{\partial \psi}{\partial x}$.

Then the equations (11) and (13) transformed to the following non dimensional forms, respectively:

$$f''' + \frac{16+15x}{20(1+x)} ff'' - \frac{6+5x}{10(1+x)} f'^2 - Mx^{2/5}(1+x)^{1/10} f' + h = x\left(f'\frac{\partial f'}{\partial x} - f''\frac{\partial f}{\partial x}\right) \tag{17}$$

$$\frac{1}{\Pr} h'' + \frac{16+15x}{20(1=x)} fh' - \frac{1}{5(1+x)} f'h + Nxf''^2 + Jx^{\frac{7}{5}}(1+x)^{-\frac{1}{2}} f'^2$$
$$-\varepsilon\left\{\left(\frac{1+x}{x}\right)^{1/5}\left(\frac{T_\infty}{T_b - T_\infty}\right) f' + hf'\right\} = x\left(f'\frac{\partial h}{\partial x} - h'\frac{\partial f}{\partial x}\right) \tag{18}$$

In the above equations the primes denote differentiation with respect to η. The boundary conditions (14)-(15), take the following forms:

$$f(x,0) = f'(x,0) = 0, h'(x,0) = -(1+x)^{1/4} + x^{1/5}(1+x)^{1/20} h(x,0)$$
$$f'(x,\infty) = 0\ ,\ h'(x,\infty) = 0 \tag{19}$$

The solutions of the above equations (17) and (18) together with the boundary conditions (19) enable us to calculate the skin friction τ and the surface temperature θ (x, 0) from the following expressions.

$$\tau = \mu x^{2/5} (1+x)^{-3/20} f''(x, 0) \tag{20}$$

$$\theta = x^{1/5} (1+x)^{-1/5} h(x, 0) \tag{21}$$

METHOD OF SOLUTION

The numerical methods used is finite difference method together with Keller box Scheme by Keller[12]. To begin with, the partial differential Eqs. (17)-(18) are first converted into a system of first order differential equations. Then these equations are expressed in finite difference forms by approximating the functions and their derivatives in terms of the central difference formula. Denoting the mesh points in the (x,η)-plane by x_i and η_j where i = 1, 2, . . . , M and j = 1, 2, . . . , N, center difference approximations are made, such that those equations involving x explicitly are centered at ($x_{i-1/2}$, $\eta_{j-1/2}$) and the remainder at (x_i , $\eta_{j-1/2}$), where $\eta_{j-1/2} = \frac{1}{2}(\eta_j + \eta_{j-1})$ etc. The above central difference approximations reduce the system of first order differential equations to a set of non-linear difference equations for the unknown at x_i in terms of their values at x_{i-1}. The resulting set of nonlinear difference equations are solved by using the Newton's quasi-linearization method. The Jacobian matrix has a block-tridiagonal structure and the difference equations are solved using a block-matrix version of the Thomas algorithm; the details of the computational procedure have been discussed further by Cebecci and Bradshow[13] and widely used by Hossain and Alim[14] and Hossain et al.[15].

RESULTS AND DISCUSSION

Solutions are obtained for Prandtl number, Pr = 0.1, 0.72, 1.0,1.74, the viscous dissipation parameter, N = 0.1, 0.4, 0.7, 1.0 and the Joule-heating parameter, J =0.1, 0.3, 0.6, 0.8. We used another pressure work parameter ε = 0.1, 0.4, 0.7, 0.9. If we know the values of the functions f (x, η), h (x, η) and their derivatives for different values of the Prandtl number Pr and the Joule-heating parameter J, we may calculate the numerical values of the surface temperature θ (x, 0) and the velocity gradient f'' (x, 0) at the surface that are important from the physical point of view.

Fig.2 (a) and Fig.2 (b) deal with the effect of the viscous dissipation parameter N (= 0.10, 0.40, 0.70, 1.00) on velocity and temperature distributions at Pr = 0.72, J = 0.7 and ε = 0.4. From Fig. 2(a), it is revealed that the velocity profile $f'(x, \eta)$ moves slightly upward with the increase of the viscous dissipation parameter N which indicates that viscous dissipation enhances the fluid motion slightly. In Fig.2 (b), it is shown that the temperature profile h (x, η) is influenced by the increasing values of N at small values of η.

It is seen from Fig. 3(a) that an increase in the Joule heating parameter is associated with a considerable increase in velocity. Near the surface of the plate (small η) the velocity increases, becomes maximum, then decreases and finally (large η) approaches to zero. The maximum values of the nondimensional velocities $f'(x, \eta)$ are 0.4251, 0.4428, 0.5213, 0.5542 for J = 0.10, 0.30, 0.60, 0.80 respectively and each of which occurs at η = 1.3025 for the first maximum value and η = 1.3693 for the 2nd, 3rd and 4th maximum values. Here, it is observed that the $f'(x, \eta)$ increases by 30.37% as J increases from 0.1 to 0.8. Fig. 3(b) shows the distribution of the temperature profiles h (x, η) against η for the same values of the Joule heating parameter J and each of which reaches the maximum at the surface. Thus h (x, η) increases by 16.23% as J increases from 0.10 to 0.80.

Fig. 4 (a) and 4(b) deal with the effect of the pressure

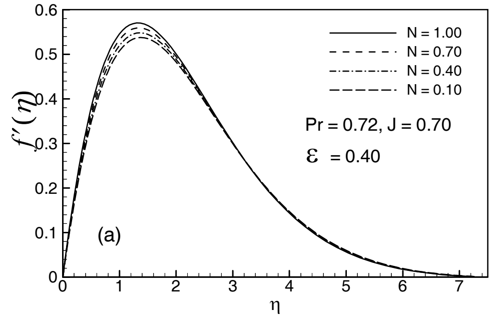

Figure 2a: Variation of dimensionless velocity profiles $f'(x,\eta)$ with dimensionless distance η for different values of viscous dissipation parameter *N*.

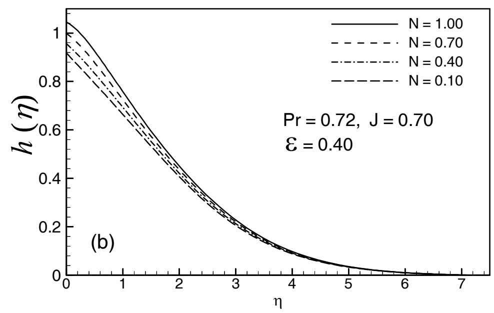

Figure 2b: Variation of dimensionless temperature profiles $h\,(x,\eta)$ against dimensionless distance η for different values of viscous dissipation parameter *N*.

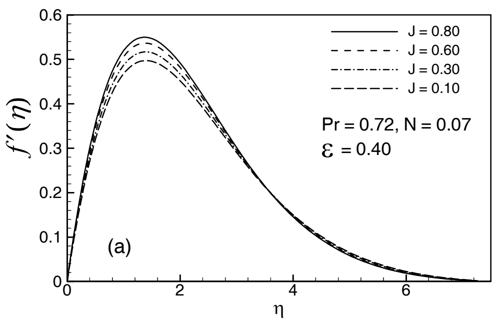

Figure 3a: Variation of dimensionless velocity profiles $f'(x,\eta)$ against dimensionless distance η for different values of Joule heating parameter *J*.

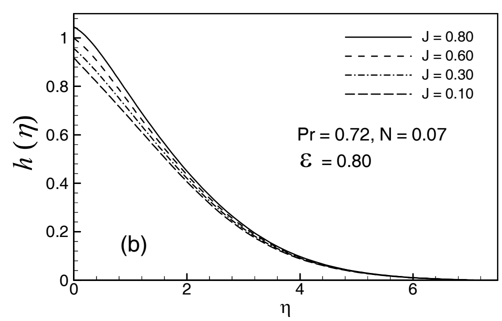

Figure 3b: Variation of dimensionless temperature profiles $h\,(x,\eta)$ against dimensionless distance η for different values of Joule heating parameter *J*.

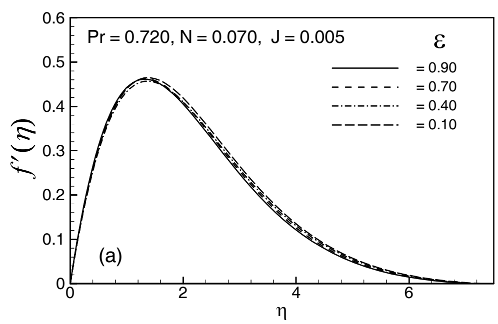

Figure 4a: Variation of dimensionless velocity profiles $f'(x,\eta)$ against dimensionless distance η for different values of pressure work parameter $\in$.

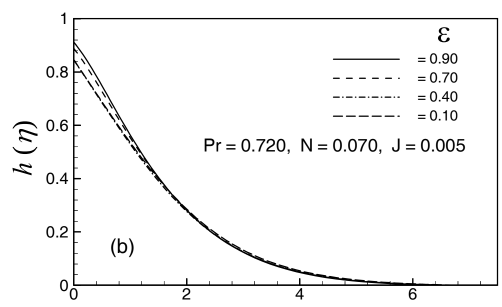

Figure 4b: Variation of dimensionless temperature profiles $h\,(x,\eta)$ against dimensionless distance η for different values of pressure work parameter $\in$.

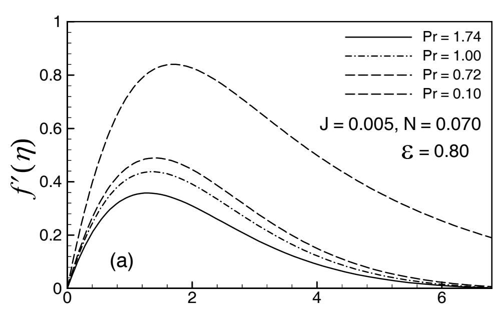

Figure 5a: Variation of dimensionless velocity profiles $f'(x,\eta)$ against dimensionless distance η for different values of Prandtl number *Pr*.

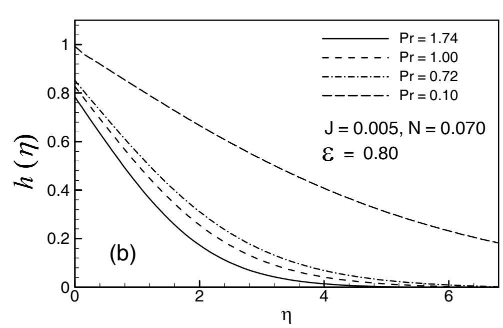

Figure 5b: Variation of dimensionless temperature profiles $h\,(x,\eta)$ against dimensionless distance η for different values of Prandtl number *Pr*.

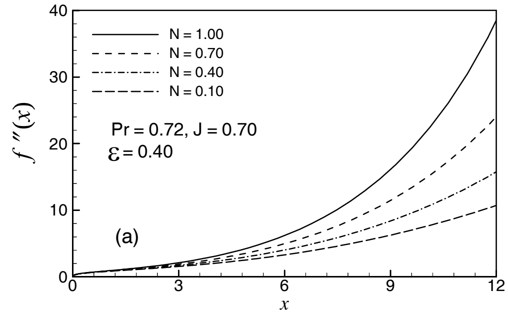

Figure 6a: Variation of skin friction coefficient $f''(x, 0)$ with dimensionless distance x for different values of viscous dissipation parameter N.

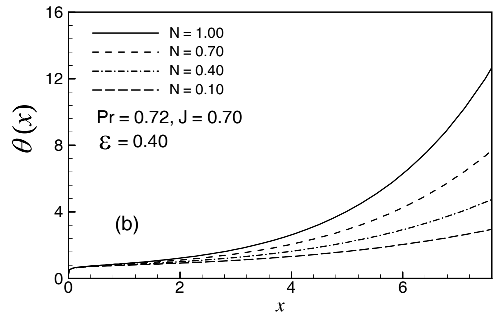

Figure 6b: Variation of surface temperature $\theta(x, 0)$ with dimensionless distance x for different values of viscous dissipation parameter

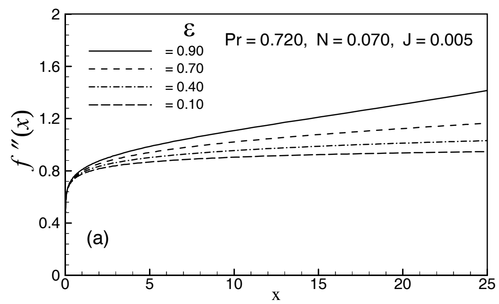

Figure 7a: Variation of skin friction coefficient $f''(x, 0)$ with dimensionless distance x for different values of pressure work parameter $\in$.

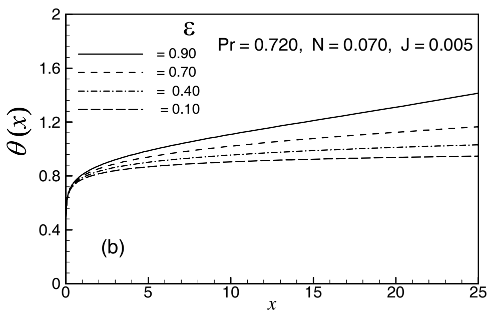

Figure 7b: Variation of surface temperature $\theta(x, 0)$ with dimensionless distance x for different values of pressure work parameter $\in$.

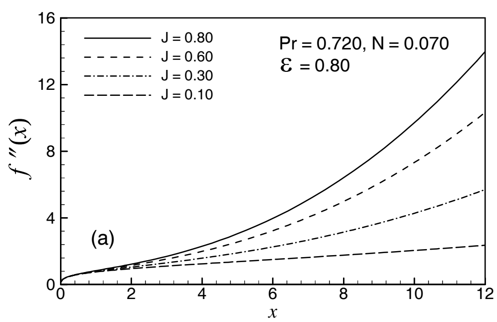

Figure 8a: Variation of skin friction coefficient $f''(x, 0)$ with dimensionless distance x for different values of Joule heating parameter J.

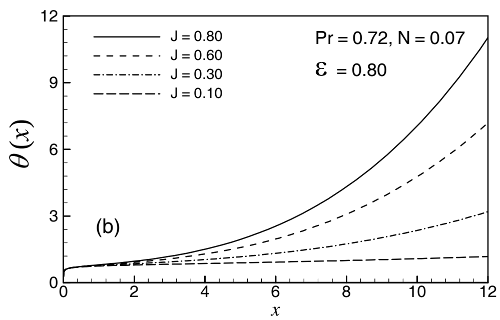

Figure 8b: Variation of surface temperature $\theta(x, 0)$ with dimensionless distance x for different values of Joule heating parameter J.

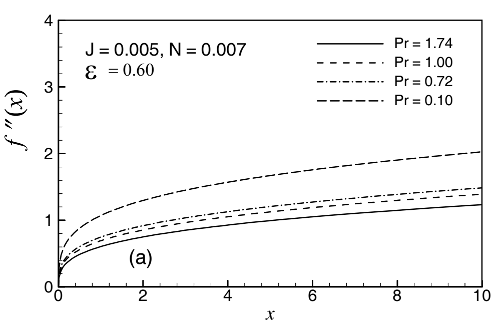

Figure 9a: Variation of skin friction coefficient $f''(x, 0)$ with dimensionless distance x for different values of Prandtl number Pr.

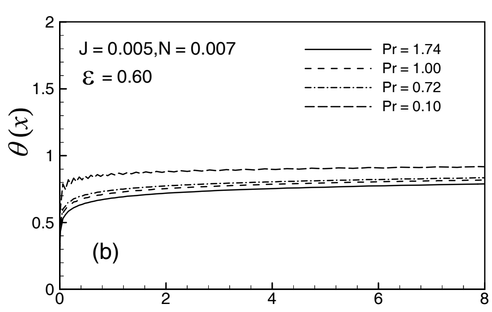

Figure 9b: Variation of surface temperature $\theta(x, 0)$ with dimensionless distance x for different values of Prandtl number Pr.

work parameter ε (= 0.1, 0.4, 0.7, 0.9) on velocity and temperature distributions at Pr = 0.72, N = 0.07 and J = 0.005 on the velocity profile $f'(x, \eta)$ and the temperature profile $h(x, \eta)$. From Fig. 4(a), it is revealed that the velocity, $f'(x, \eta)$ changes very small with the increase of the pressure work parameter ε which indicates that the influence of the pressure work parameter on the fluid motion is insignificant. Fig. 4(b) shows that the temperature profiles $h(x, \eta)$ are also insensitive to the increasing values of pressure work parameter ε.

Fig. 5(a) depicts the velocity profile for different values of the Prandtl number, Pr (= 0.10, 0.72, 1.0, 1.74) for N = 0.07, J = 0.005 and ε = 0.80. Corresponding distribution of the temperature profile $h(x, \eta)$ in the fluids is shown in Fig. 5(b). From Fig. 5(a), it is seen that if the Prandtl number increases, the velocity of the fluid decreases. On the other hand, from Fig. 5(b) it is observed that the temperature decreases within the boundary layer due to increase of the Prandtl number Pr.

Numerical values of the velocity gradient $f''(x, 0)$ and the surface temperature $\theta(x, 0)$ are depicted graphically in Fig.6 (a) and 6(b), respectively against the axial distance x for different values of the viscous dissipation parameter N (=0.1, 0.4, 0.7, 1.0) for the fluid having Prandtl number Pr = 0.72. It is seen from Fig. 6(a) that the skin-friction $f''(x, 0)$ increases when the viscous dissipation parameter, N increases. It is also observed in Fig. 6(b), that the same result holds for surface temperature $\theta(x, 0)$ distribution.

From Fig. 7(a), it is observed that increase in the value of the pressure work parameter ε leads to increase of the value of the shear stress coefficient $f''(x, 0)$ which is usually expected. Again from Fig. 7(b) it is illustrated that the increase of the pressure work parameter ε leads to increase of the surface temperature $\theta(x, 0)$.

The effect of Joule heating parameter J (= 0.1, 0.3, 0.6, 0.8) on the skin-friction $f''(x, 0)$ and the surface temperature distribution $\theta(x, 0)$ against x for Pr = 0.72, N = 0.70 and ε = 0.80 is shown in Fig. 8(a)-8(b). It is found that the values of the skin-friction $f''(x, 0)$ and the surface temperature distribution $\theta(x, 0)$ both increases for increasing values of Joule heating parameter J. Here, it has been observed that the values of the skin-friction $f''(x, 0)$ increases by 76.73% and the surface temperature $\theta(x, 0)$ increases by 83.26% while J increased from 0.10 to 0.80.
From Fig. 9(a), it is be observed that increase in the value of the Prandtl number Pr (= 0.1, 0.72, 1.0, 1.74) leads to decrease of the value of shear stress $f''(x, 0)$. Similar results hold in surface temperature distribution $\theta(x, 0)$ shown in Fig. 9(b) for the same values of Prandtl number Pr at J = 0.005, N = 0.007 and ε = 0.60.

Numerical values of the shear stress coefficient and the surface temperature distribution for different values of the Prandtl number Pr while N = 0.007, ε = 0.60 and J = 0.005 are shown in Table 1. From Table 1, it is found that the values of skin friction coefficient decrease at different position of x for Prandtl number Pr = 0.1, 0.72, 1.0, 1.74. Near the axial position x = 3.1340, the rate of decrease of the local shear stress coefficient is 41.3763% as the Prandtl number Pr changes from 0.1 to 1.74. Furthermore, it is seen that the numerical values of the surface temperature decrease for increasing values of Prandtl number Pr. This suggests that the interface of the plate having thickness 'b' remains heated more in the fluid with lower Prandtl number than that of the higher Prandtl number and at the same axial position x = 3.1340, the rate of decrease of surface temperature is 17.1856% as the Prandtl number changes from 0.1 to 1.74.

CONCLUSIONS

The effect of viscous dissipation N and pressure work parameter ε for Prandtl number Pr (= 0.1, 0.73, 1.0, 1.74) on natural convection boundary layer flow along a vertical flat plate has been studied introducing a new class of transformations. The transformed non-similar boundary layer equations governing the flow together with the boundary conditions based on conduction and convection were solved numerically using the implicit finite difference method together with Keller box scheme. The coupled effect of natural convection and conduction required that the temperature and the heat flux be continuous at the interface. From the present investigation, the following conclusions may be drawn:

- The skin friction and the velocity increase with increasing values of the viscous dissipation parameter N, the pressure work parameter ε and the Joule heating parameter J.
- Increased values of the viscous dissipation parameter N leads to increase in the surface temperature as well as the velocity.
- Increased values of the pressure work parameter ε do not affect the surface temperature significantly.
- Increased values the Joule heating parameter J leads to increase in the surface temperature as well as the velocity.
- The skin friction coefficient, the surface temperature and the velocity decrease over the whole boundary layer with the increase of the Prandtl number Pr.

REFERENCES

1. Ackroyd, J. A. D., "Stress work effects in laminar flat-plate natural convection", *J. Fluid Mech.*, 62, pp.677- 695, 1974.
2. Alam, Md. M., Alim, M. A., and Chowdhury, Md. M. K., "Free convection from a vertical permeable circular cone with pressure work and non-uniform surface temperature", *Nonlinear Analysis; Modelling and Control*, Vol.12, No.1, pp.21-32, 2007.
3. Alam, Md. M., Alim, M. A., and Chowdhury, Md. M. K., "Effect of pressure stress work and viscous dissipation in natural convection flow along a vertical flat plate with heat conduction", *J. Naval Arch. and Marine Engineering,* Vol.3, No.2, pp. 69-76, 2006.
4. Alim, M. A., Alam, Md. M., Mamun, A. A. and Hossain, B., "Combined effect of viscous dissipation and Joule heating on the coupling of conduction and free convection along a vertical flat plate", *Int. Comm. of heat and mass transfer,* 2007, DOI: 10.1016/j.icheatmasstransfer. 2007.06.003.

5. Gebhart, B., “Effects of viscous dissipation in natural convection”. *J. Fluid Mech*. Vol.14, pp. 225-232, 1962.
6. Joshi, Y. and Gebhart, B., “Effect of pressure stress work and viscous dissipation in some natural convection flows”, *Int. J. Heat Mass Transfer*, 24(10), pp. 1377-1388, 1981.
7. Miyamoto. M., Sumikawa. J., Akiyoshi, T. and Nakamura, T., “Effect of axial heat conduction in a vertical flat plate on free convection heat transfer”, *Int. J. Heat Mass Transfer*, 23**,** pp.1545-1533, 1980.
8. Pozzi, A. and Lupo, M., “The coupling of conduction with laminar natural convection along a flat plate”, *Int. J. Heat Mass Transfer* 31(9), pp. 1807-1814, 1988.
9. Takhar, H. S. and Soundalgekar, “V. M., Dissipation effects on MHD free convection flow past a semi-infinite vertical plate”, *Applied Scientific Research*. 36, pp.163-171, 1980.
10. Sparrow, E. M. and Cess, R. D., “The effect of a magnetic field on free convection heat transfer”, *Int. J. Heat Mass Transfer,* 3, pp.267-274, 1961.
11. Zakerullah, Md. “Viscous dissipation and pressure work effects in axisymmetric natural convection flows”. *Ganit* (*J. Bangladesh Math. Soc*.) Vol. 2(1), pp.43-51, 1972.
12. Keller H. B., “ Numerical methods in boundary layer theory”, *Annual Rev. Fluid Mech*., 10, pp.417-443, 1978.
13. Cebeci, T. and Bradshaw, P., “Physical and Computational Aspects of Convective Heat Transfer”, *Springer*, N. Y. 1984.
14. Hossain, M. A. and Alim**,** M. A., “Natural convection-radiation interaction on boundary layer flow along a Thin cylinder”, *J. Heat and Mass Transfer* 32, pp.515-520, 1997.
15. Hossain, M. A., Alim**,** M. A. and Rees, D. A. S. “Effects of thermal radiation on natural convection over cylinders of elliptic cross section.” Acta Mechanica, 129**,** pp.177-186, 1998.